PERIODICO di MINERALOGIA
established in 1930

DIPARTIMENTO
DI SCIENZE DELLA TERRA

SAPIENZA
UNIVERSITÀ DI ROMA

An International Journal of
Mineralogy, Crystallography, Geochemistry,
Ore Deposits, Petrology, Volcanology
and applied topics on Environment, Archaeometry and Cultural Heritage

Mineralogical and petrogenetic characteristics of the peridotites and associated podiform chromitites from Abgarm ultramafic complex (south-eastern Iran)

Raziyeh Alipour [1], Hesam Moeinzadeh [1,*], Cristina Perinelli [2], Ferdinando Bosi [2], Hamid Ahmadipour [1]

[1] Department of Geology, Shahid Bahonar University, Kerman, Iran
[2] Department of Earth Sciences, Sapienza Università di Roma, Italy

ARTICLE INFO

Submitted: November 2020
Accepted: May 2021
Available on line: July 2021

* Corresponding author:
hesammoeinzadeh@yahoo.com

Doi: 10.13133/2239-1002/17215

How to cite this article:
Alipour R. et al. (2021)
Period. Mineral. 90, 341-357

ABSTRACT

Abgarm ultramafic complex is a part of the Esfandagheh-Hajiabad coloured melange belt located in the south east of the Iranian segment of Alpine-Himalayan orogenic belt. The complex has faulted contacts with flysch-type sediments of the upper cretaceous ophiolite melange complex. Although Harzburgite is the dominant lithotype, dunites and lherzolites occur in lesser extents, where some dunites contain massive chromitite pods or bands. The chemistry of minerals of harzburgite samples reflects the depleted nature of these rocks and indicates that the Abgarm mantle peridotites experienced a melt extraction of less than 30%. Geothermo-barometric estimates indicate that the Abgarm harzburgites initially equilibrated at temperatures between 809-923 °C and then they re-equilibrated at 613-725 °C, in a range of pressures of 1.1 and 2.3 GPa. Moreover, fO_2 calculation for these rocks gives a redox state (Δlog=0.1-0.7 log-bar units) above the fayalite-magnetite-quartz buffer.

Tectonomagmatic discrimination diagrams based on mineral compositions depict that Abgarm harzburgites and lherzolites evolved as abyssal peridotites, which shows a tendency towards SSZ peridotites and also reflects that they probably were formed in a back-arc basin environment. Dunites and chromitites of the complex can be produced by the reaction of the back-arc basin basaltic melts with the mantle peridotites.

Keywords: Abgarm ultramafic complex; Esfandagheh-Hajiabad coloured melange; Harzburgite; Chromitite; Boninite; subduction zone.

INTRODUCTION

An ophiolite represents fragments of oceanic lithosphere and upper mantle emplaced tectonically along continental margins in accretionary prisms during orogenic processes. They provide significant information on the evolutionary history of ancient oceanic crust and mantle beneath spreading centers in mid-ocean ridge (MOR) and supra-subduction zone (SSZ) tectonic settings (Pelletier et al., 2008; Ahmed, 2013; Dai et al., 2013; Dilek and Furnes, 2014). In particular, ophiolitic peridotites are a product of partial melting and the melt-rock reactions that are strongly controlled by variations in temperature, pressure, fluid flux, and oxygen fugacity in the upper mantle (Parkinson and Pearce 1998; Niu, 2004; Dupuis et al, 2005; Dilek and Furnes, 2014; Zhang et al., 2016; Lian et al., 2016; Singh et al., 2017; Lian et al., 2019). Therefore, the mineral forming the ophiolitic peridotites and their modal proportions, mineral, and whole-rock chemistry

are significant indicators of the physical conditions and tectonic settings of ophiolite formation (Dilek and Furnes, 2014). Generally, Ophiolitic peridotites in different tectonic settings have undergone distinct geological processes. For example, decompression melting of mantle rocks at low oxygen fugacity (fO_2) conditions could happen in a mid-ocean ridge setting, while the interactions between refractory mantle and volatile-rich boninite usually occur in supra-subduction zone settings (SSZ) at high fO_2 conditions (Uysal et al., 2016). As suggested by Weber- Diefenbach et al., (1984) and Arvin and Robinson, (1994), the Iranian ophiolites are divided into those of Paleozoic and Mesozoic. The latter are the most abundant and include the Abgarm ultramafic complex. The Iranian parts of the Alp-Himalayan orogeny include several remnants of Neotethyan oceanic basin (Shafaii Moghadam et al., 2012) (Figure 1a). Neotethyan ophiolites in Iran form important parts of the 3000 Km long ophiolite-rich zone that extends from Troodos (Cyprus) through Turkey eastwards as far as Semail (Oman; Shafaii Moghadam and Stern, 2015). These ophiolite complexes have been studied by several researchers (e.g., Moores et al., 2000; Robertson, 2002; Dilek and Furnes, 2009; Pearce and Robinson, 2010).

The Abgarm ultramafic complex (Kerman province, Iran) and its major rock units (harzburgites, lherzolites, dunites, and chromitites) are one of several ultramafic complexes in the highly faulted Haji-Abad ophiolite belt, which were formed in the late Cretaceous (Shafaii Moghadam et al., 2012). Many academic works and studies done on this belt have proved that the ultramafic complexes belong to the supra-subduction zone setting (Peighambari et al., 2011; Jannessary et al., 2012; Najafzadeh and Ahmadipour, 2014; Mohammadi et al., 2018). Based on studies on spinels and olivines from the Abgarm peridotites by Alipour et al. (2021a, 2021b), It is inferred that the rocks in this complex were formed in a back-arc basin environment. Whereas, in the present study we extend the work of Alipour et al. (2021a, 2021b) by expanding the analytical dataset and considering all mineral phases. In particular, the purpose of this study is to report the field relations, the petrographical and mineralogical characteristics along with the presentation of geochemical data and oxidation state conditions in Abgarm upper mantle rock units for the first time and also to understand the evolution of this complex based on mineral chemistry.

ANALYTICAL METHODS

Among the freshest samples, lithotypes representing harzburgite (8 samples), dunite (2 samples), lherzolite (2 samples), websterite (1 sample), and chromitite (2 samples) have been selected for the chemical analyses. The mineralogical and textural characteristics of the selected samples were studied through optical and scanning electron microscopes (SEM). SEM images were obtained using an FEI Quanta-400 scanning electron microscope equipped with an EDAX Genesis microanalysis, which is available at the Department of Earth Sciences of Sapienza University of Rome. Mineral compositions were determined with a Cameca SX50 electron microprobe of the CNR-Istituto di Geologia Ambientale e Geoingegneria (Rome), at the Department of Earth Sciences of Sapienza University of Rome. The electron microprobe is equipped with five wavelengths dispersive spectrometer (WDS) and the quantitative analyses were performed using 15 kV accelerating voltage and 15 nA beam current. Regarding standards, we took advantage of pure metals for Mn and Cr, jadeite for Na, wollastonite for Si and Ca, orthoclase for K, corundum for Al, magnetite for Fe, rutile for Ti, and periclase for Mg. Counting times were 20s for elements, 10s for backgrounds, and a beam diameter of 1 μm. As a correction routine, we used the PAP method (Pouchou and Pichoir, 1991).

Furthermore, some analyses were performed on minerals with a JEOL- JXA-8600M electron microprobe analyzer at 15Kv accelerator voltage and 20nA rays at the Department of Earth and Environmental Sciences at the University of Yagamata, Japan.

GEOLOGICAL SETTING

Abgarm ultramafic complex is a part of peridotite bodies of the late Cretaceous Esfandagheh-Haji Abad ophiolite mélange belt. This belt and its associated arc-related rocks are located in the southeast of the Iranian segment of ~~the~~ Alpine-Himalayan orogenic belt and cover about 2000 km^2 near the main Zagros thrust fault (Shafaii Moghadam et al., 2012). Haji Abad ophiolite has tectonic contacts with the high-pressure blue-schists of the Sanandaj Sirjan zone, dated 85- 95 Ma (Agard et al., 2006). Two groups of ophiolitic mélange units can be identified in the Esfandagheh-Haji Abad region: the older upper Triassic-Cretaceous one, which occurs in the north (Sikhoran-Soghan subduction-accretion mélange, Ghasemi et al., 2002; Ahmadipour et al., 2003) and in the south the younger one, late Cretaceous Haji Abad ophiolites, near the main Zagros trust (Shafaii Moghadam et al., 2012). Concerning Haji Abad ophiolite, the main lithology is constituted by mantle tectonites (mostly lherzolites, depleted harzburgite with widespread residual and foliated/ discordant dunite lenses). Podiform chromitites are common and are usually enveloped by thin dunitic haloes, which are thought to be reflecting channelled and/ or porous flow of boninitic melt and reactions with wall-rock peridotite (Keleman et al., 1992). Instead, the crustal sequences are characterized by ultramafic cumulates, a

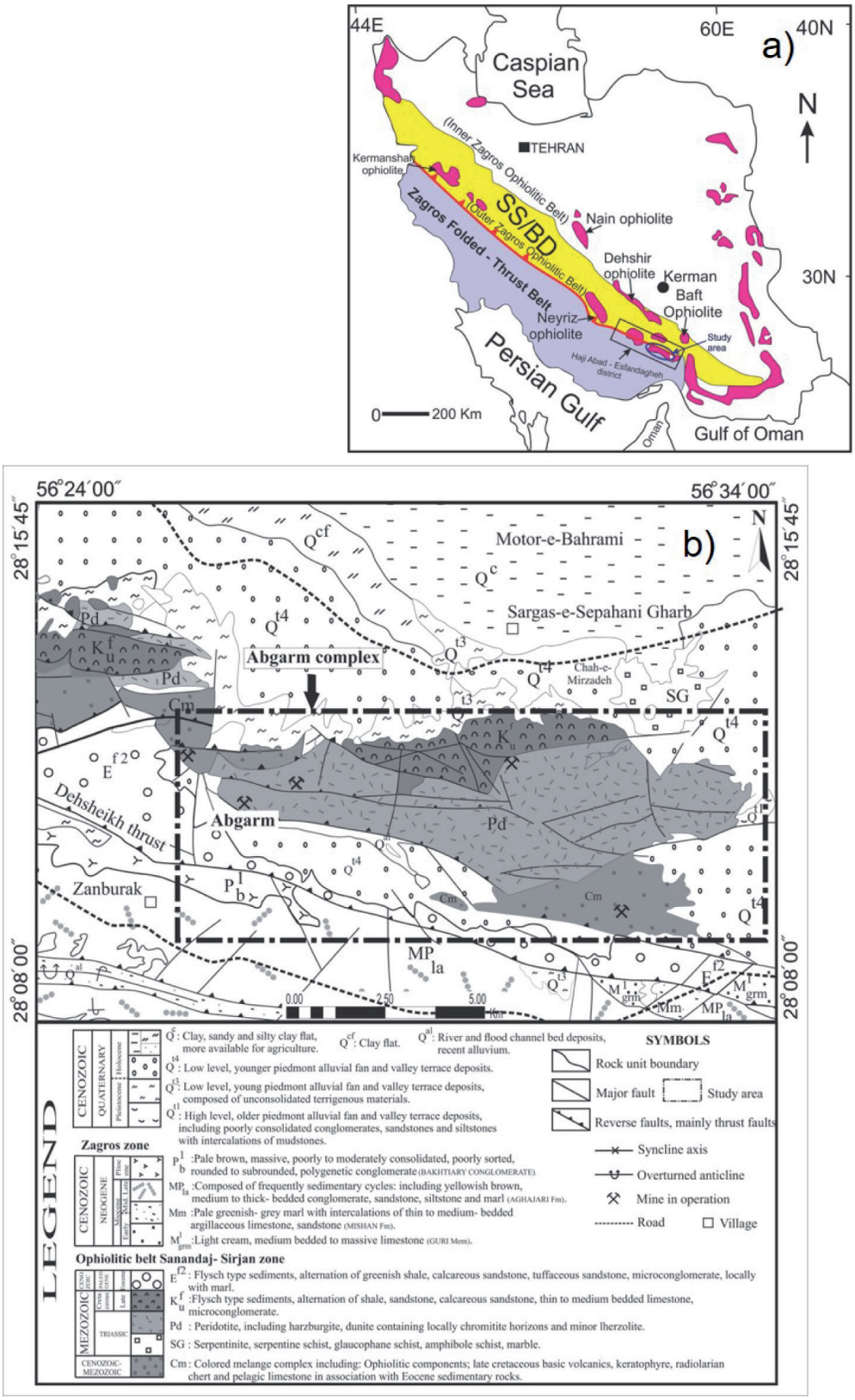

Figure 1. a) Location of the study area within the Iranian ophiolitic belts (modified after Shafaii Moghadam and Stern, 2015); b) Geological map of Abgarm region adapted from the map of the 1:100,000 Orzueiyeh and Dolat Abad (after Sahandi et al., 2007).

volcanic pile, and cumulate rocks constituted by dunites, chromitites, lherzolite, pyroxenite, and wherlite (Shafaii Moghadam et al., 2012).

Abgarm complex is about 20 km by 4 km wide. In the north and north-west sides, the complex has faulted contacts with flysch type sediments of the upper cretaceous ophiolite melange complex. whereas, in the south part, the complex probably has fault contacts with the quaternary alluvial deposits (Figure 1b). This complex, the same as other ultramafic-mafic complexes in the Esfandagheh region, has been interpreted as an Alpine-type peridotite representing one of remnant parts of the Paleaotethys within an Upper Cretaceous ophiolite mélange within the Zagros thrust zone (e.g., Ahmadipour et al., 2003; Jannessary et al., 2012; Najafzadeh and Ahmadipour, 2014; Shafaii Moghadam and Stern, 2015; Khalatbari Jafari et al., 2016; Peighambbari et al., 2016).

FIELD RELATIONSHIPS

The Abgarm complex contains harzburgite, dunite, lherzolite, pyroxenite dykes (Figure 2 a-d), and chromitite lenses, in which nearly all contacts are faulted and serpentinized. Harzburgite is the main lithology and constitutes about 80% of the complex, which appear as homogenous coarse-grained outcrops without distinct layering or foliation. The main part of these rocks is formed by interlocking massive olivine grains. Besides, there is a great deal of shiny orthopyroxene (Opx) crystals appearing on the surface of the samples (Figure 2e). Dispersed small grains of spinels also characterize the harzburgite surfaces. Harzburgites show sharp and faulted contacts with all rock units, where the highest degrees of serpentinization occurred; some fractures have been filled with magnesite veins (Figure 2 f,g). Lherzolites are gray and mainly found in the margins of the complex and their contact with harzburgites are often sharp, tectonized, and serpentinized. They are generally coarse-grained rocks without any foliation and make up about 10% of the Abgarm massif. Dunites form small to large irregular bodies in the complex and some of them contain chromitite ore deposits. The chromitites have a variety of textures like massive, banded, and disseminated (Figure 2 g,i).

PETROGRAPHY

According to petrographic studies and mineral modals determined, the olivine-orthopyroxene-clinopyroxene diagram (Le Maitre, 1989) was used in order to decide the type of rocks and the position of different rocks identified on it (Figure 3). Harzburgite is the dominant lithology of Abgarm complex, which contain 65-85 vol% olivine, 12-23 vol% orthopyroxene ,1-3 vol% of clinopyroxene and about 2 vol% spinel.

The common texture of these rocks is proto-granular, although the porphyroclastic type also frequently occurs. Three generations of olivines have been recognized: the first generation olivines (Ol1) are large grains (up to 5 mm in size) with a porphyroclastic texture and sometimes have mechanical twining. Besides, the evidence of grain boundary migration can be observed in these rocks. Boundaries between these crystals are commonly slightly curved, irregular, and sometimes stretching due to the dynamic recrystallization (Figure 4 a,b). Due to high-temperature deformation processes, crystals display elongation, more curved/sinusoidal boundaries, and irregular shapes. Small olivines (Ol2; <1 mm in size) occur around or within orthopyroxene porphyroclasts (Figure 4a). They show polygonal shapes with triple-junction boundaries and are devoid of any deformation features. The third generation of olivines (Ol3) aggregates were formed between or within the large orthopyroxenes porphyroclasts (Figure 4 a,b).

Two generations of orthopyroxene are also recognized: the first one (Opx1) is colorless, semi-rounded, and large porphyroclasts with a size of over 1 cm and often retains deformational features such as being slightly folded, kink band, clinopyroxene exsolution lamellae, and elongation (Figure 4 a,b). The second type of orthopyroxene (Opx2) is crystallized as mosaic textured un-deformed crystals, which were formed along olivine-olivine grain boundaries. (Figure 4b). Clinopyroxenes is interstitial to orthopyroxene or olivine grains. Spinels in harzburgite are brown colored and can be divided into two groups based on their shape. The first type of spinel (Sp1) is formed as coarse-grained independent crystals inside or around the olivines and orthopyroxenes; they have subidiomorphic shapes with pull-apart fractures (Figure 4d). The second type of spinels (Sp 2) occurs as small-grained anhedral crystals. They have been formed between orthopyroxene and olivine grains (Figure 4e). Occasionally, Fe-rich oxide is formed along with fractures and rims of Cr-spinels, and minor amounts of sulfide also occur in close textural association with the crystals, usually separated from fresh Cr-spinel by sieve textured coronas (Figure 4f).

The lherzolites of Abgarm ultramafic complex contain 70-75 vol% olivine, 15-20 vol% orthopyroxene, 10 vol% clinopyroxene and about 1-2 vol% spinel. Petrographically, lherzolites are very similar to the harzburgites and also contain various generations of olivine, orthopyroxene, clinopyroxene, and spinel (Figure 4c). In these rocks, olivine occurs as large porphyroclastic deformed grains (Ol1) with deformation twining and elongation, in which high-temperature deformation was recorded. As well as that, there are some small neoblastic olivine grains (Ol2) without any deformation features in these rocks, which have been formed around orthopyroxene and olivine

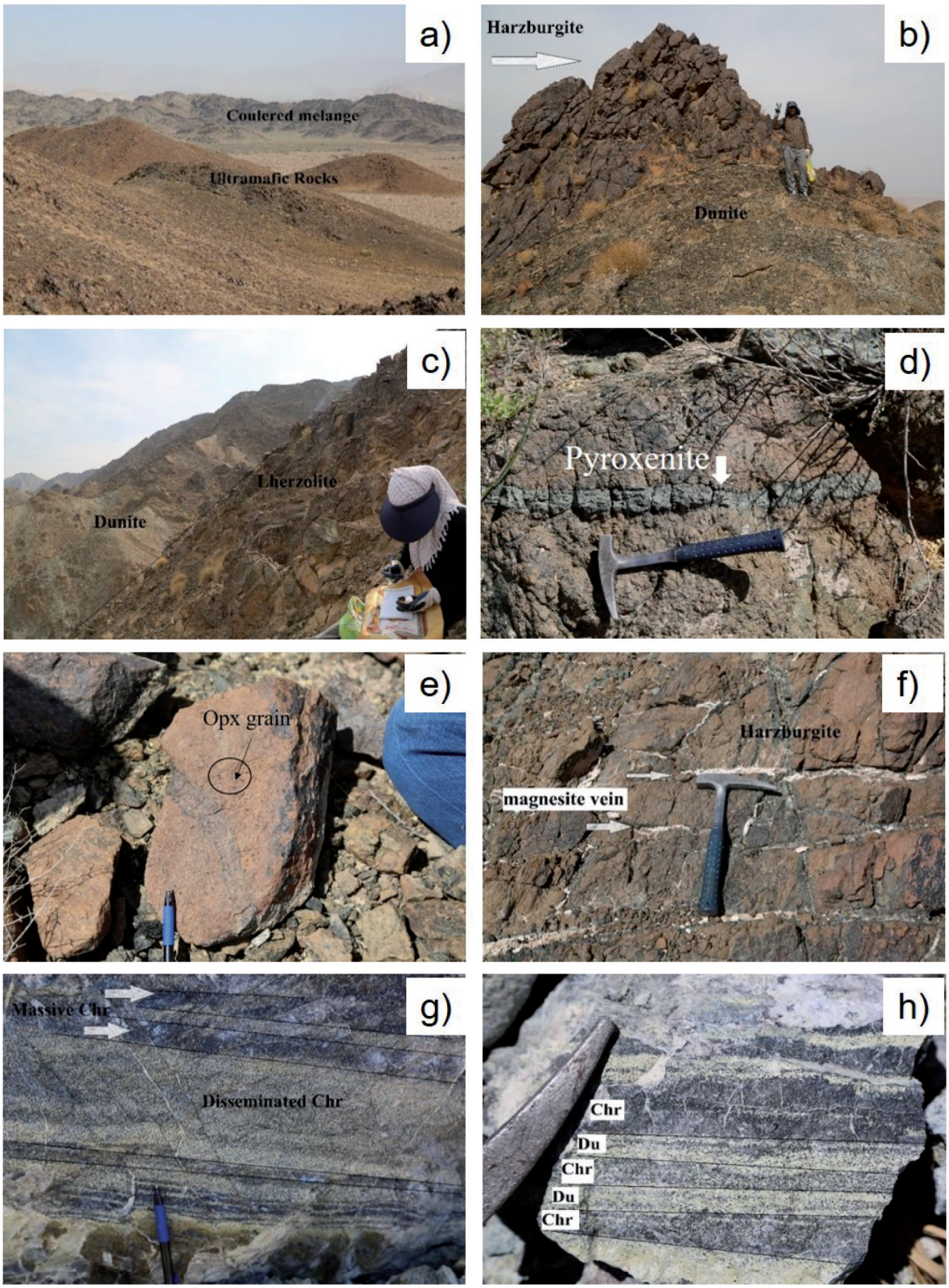

Figure 2. a) General view of the Abgarm ophiolite;. b) Contact of harzburgite and dunite in the Abgarm complex; c) A view of dunite and lherzolite contact; d) Pyroxenite dyke in harzburgite; e) Coarse grains of orthopyroxene in the harzburgite; f) Magnesite veins in the harzburgite; g) Chromites disseminated in dunites associated with h) Chromitite (Chr) layers in dunite.

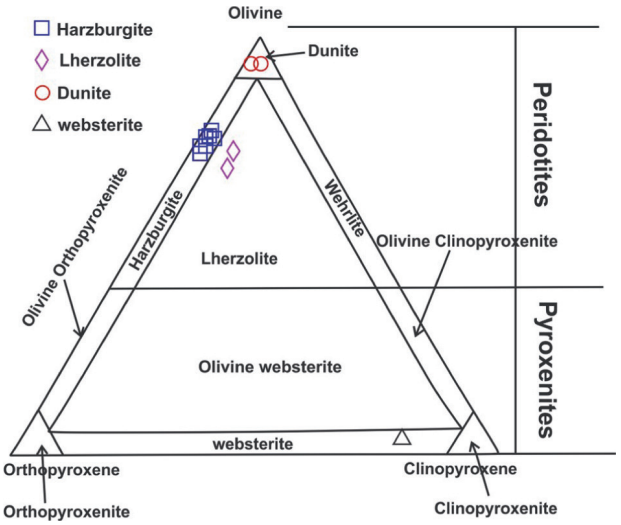

Figure 3. Position of different rocks of Abgarm ultramafic complex on the distribution diagram of ultramafic rocks (Le Maitre, 1989).

porphyroclasts. The third generation of olivines (Ol3) occurs as small grain aggregates which have been formed within or between orthopyroxene porphyroclasts. These rocks also have two generations of clinopyroxenes. The first one (Cpx1) is coarse-grained crystals up to 4 mm in diameter. They exhibit deformation evidence and show curved boundaries filled with olivine, spinel, or orthopyroxene. The second-generation (Cpx2) is undeformed anhedral and inter-granular grains found around the orthopyroxene crystals. Orthopyroxene occurs either as deformed coarse-grained porphyroclast (up to 8 mm in size) (Opx1) or neoblastic undeformed between those of the first generation, which were probably formed by recrystallization processes. Spinel also occurs as two groups. The first group is independent euhedral crystals up to 1 mm in diameter, which crystallized within the olivine. These spinels are brownish-green in colour. The second group is seen as anhedral grains and crystallized between olivine and orthopyroxene grains. Pyroxenites in the study area are websterite. These rocks contain 70-75 vol% clinopyroxene, 20-25 vol% orthopyroxene, 3 vol% olivines, and less than 2 vol% spinels (Figure 4g).

Abgarm dunites consist of coarse-grained olivine in an amount of 96 % and about 4 % of spinel. These rocks display pervasive serpentinization that gives them a mesh-like texture, although their original granular texture is still recognizable. There are two types of olivines in the dunitic sample. The first type is large porphyroclastic, elongated crystals with a size varying from 1 to 2 mm (Figure 4g). Sometimes they are surrounded by undeformed smaller grains (the second type olivines; Figure 4g). These fine-grained olivines show mosaic texture and are probably formed by recrystallization of the first type of olivines at the crustal conditions.

Spinels in dunite are darker than those in harzburgite and occur along the boundaries or between olivines. Their size is between 0.5 to 2 mm and crystals sometimes show pull apart fractures and weak lineations (Figure 4h).

The studied podiform chromitite occurs as a massive type composed of ~98 of modal% spinel. Original silicate minerals in this sample are altered into serpentine. Here spinel grains are generally black euhedral to subhedral in shape and their sizes are up to 0.5 mm.

MINERAL CHEMISTRY

Olivine chemical analyses are reported in Table S1 (in Supplementary materials). Forsterite (Fo) contents of olivines in harzburgites vary a narrow range between 90.42 and 91.25. NiO contents vary between 0.33 and 0.41 wt% overlapping the range of common mantle olivines (0.25-0.51 wt% according to De Hoog et al., 2010), while MnO abundances range from 0.10 to 0.17 wt%. In the diagram Fo vs NiO diagram, the harzburgite-olivines are plotted in the field of abyssal peridotites and only some of them are within the mantle olivine array (Figure 5a). Most olivine compositions fall in the mantle olivine array (Figure 5b). Concerning harzburgite-olivines, those in dunite have higher Fo contents (93.45 on average) and NiO content (~0.46 wt%).

The amount of Fo in lherzolitic olivines ranges from 90.99 to 91.20. NiO and MnO contents vary from 0.38 to 0.45 and 0.10 to 0.17 respectively. These chemical characteristics of those olivines are similar to those of the harzburgites. In addition, in the Fo vs NiO diagram, the lherzolite-olivines are plotted in the field of abyssal peridotites.

Orthopyroxene microanalyses from the investigated ultramafic rocks are listed in Table S2 (in Supplementary materials). They consist of enstatite ($En_{91-95}Wo_1Fs_{5-8}$) with the value of Mg# varying from 90 to 94.53; the Al_2O_3 content ranges from 1.75 to 3.32 wt% while Cr_2O_3 abundance is between 0.16 and 0.45 wt%. In the Mg# vs Al_2O_3 and Mg# vs Cr_2O_3 diagrams, Abgarm orthopyroxenes are distributed between the fields of abyssal and forearc peridotites (Figure 6 a,b).

The amount of En in lherzolitic orthopyroxenes ranges from 91.15 to 92.26, while their Mg# and Al_2O_3 vary from 91.85 to 92.49 and 1.77 to 3.04 respectively. Moreover, the Cr_2O_3 content in these orthopyroxenes ranges from 0.04 to 0.18, which is less than those of harzburgites. In the Mg# vs Al_2O_3 and Mg# vs Cr_2O_3 diagrams, lherzolitic orthopyroxenes are distributed between the fields of abyssal and forearc peridotites (Figure 6 a,b).

Orthopyroxene from the Abgarm websterites shows Mg# values from 90.75 to 91.71. Al_2O_3 and Cr_2O_3 content

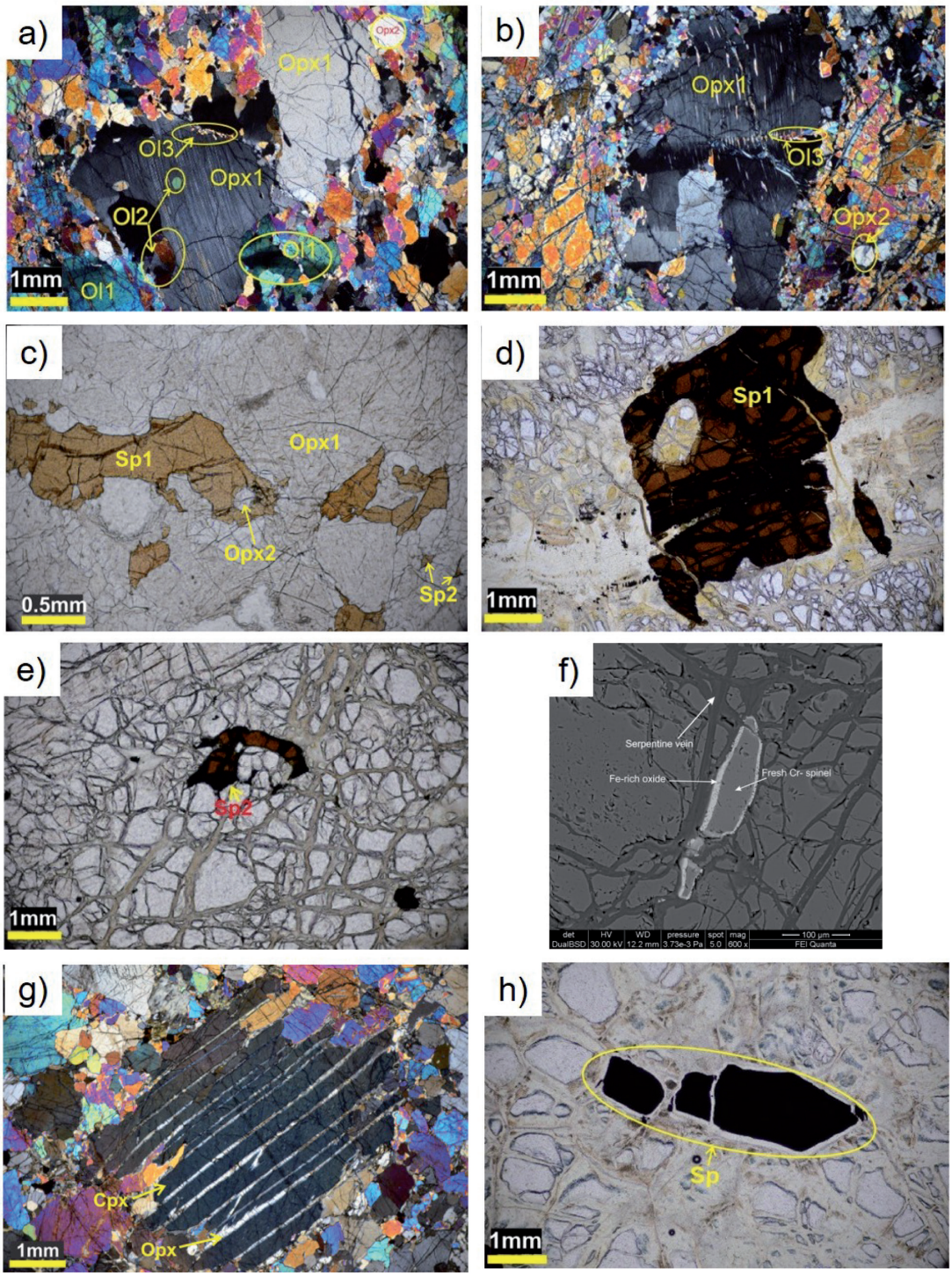

Figure 4. Microstructures of Abgarm harzburgites, lherzolites, dunites and websterite. a) and b) The different types of olivine (Ol) and orthopyroxene (Opx) in harzburgites. The first generation orthopyroxene (Opx1) while the second generation (Opx2) are represents undeformed crystals. which displays exsolution lamellae and elongation and the smaller, generally clean type 2- orthopyroxene (Opx2); c) Orthopyroxene and different generations of spinels in lherzolite; d) The first type of spinel (Sp1) formed as coarse-grained independent crystals inside or around the olivines and orthopyroxenes, they have subidiomorphic shapes with pull-apart fractures; e) The second type of spinels (Sp2) occurs as small-grained anhedral crystals and have been formed between orthopyroxene and olivine grains in harzburgites; f) Fe-rich oxide along with fractures and rims of Cr-spinels; g) Clinopyroxene with orthopyroxene exsolution lamellae in websterites; h) Spinel with pull-apart fractures and weak lineations included in the mesh textured dunite.

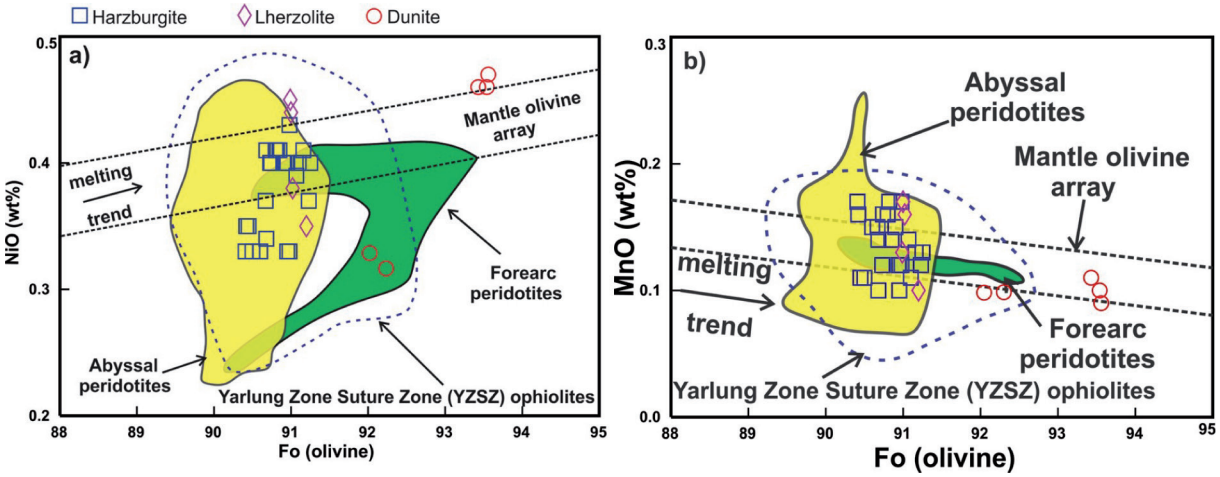

Figure 5. Compositional variations of olivines of Abgarm peridotites. Fo variations vs a) NiO and b) MnO contents. The mantle olivine array is from Takahashi et al. (1986). The fields of abyssal and forearc peridotites are from Lian et al. (2016). Dashed field outlines olivine compositions in peridotites from the Yarlung Zangpo Suture Zone (YZSZ) ophiolites after Lian et al. (2016).

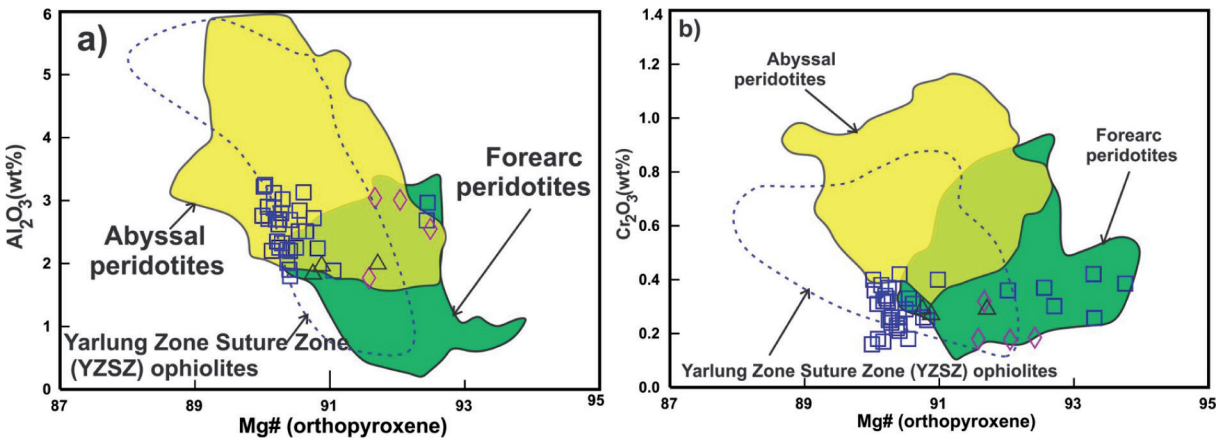

Figure 6. Compositional variations of pyroxenes from peridotites of the Abgarm peridotite complex. a) Al_2O_3 vs Mg# values in orthopyroxenes; b) Cr_2O_3 vs Mg# values in orthopyroxenes. Data of pyroxene compositions for abyssal and forearc peridotites, as well as those in peridotites from the Yarlung Zangpo Suture Zone (YZSZ) ophiolites, are from the same references used for olivines in Figure 5.

varying from 1.83 to 1.96 wt%, 0.27 to 0.29 wt%. In (Figure 6 a,b) orthopyroxenes from these rocks occur between the fields of abyssal and fore-arc peridotites.

Clinopyroxene chemical compositions are reported in Table S3 (in Supplementary materials). They are diopsides ($En_{48-50}Wo_{48-50}Fs_{1-3}$) and don't show any systematic core-rim zoning. These clinopyroxenes have low contents of Na_2O (0.11-0.22 wt%); Al_2O_3 abundances range from 2.25 to 3.51 wt%, while Cr_2O_3 varies from 0.35 to 0.57 wt%. Harzburgite-clinopyroxenes, when plotted in the discrimination Mg# vs Al_2O_3 and Mg# vs Cr_2O_3 diagrams, fall between abyssal and fore-arc peridotites or are close to the field of fore-arc peridotites (Figure 7 a,b).

Lherzolitic clinopyroxenes have En contents ranging from 47.25 to 47.95. The Wo, Fs, and Mg# contents vary from 47.43 to 48.80, from 3.95 to 5.18, and from 92.70 to 93.68 respectively. Their Al_2O_3, Na_2O, and Cr_2O_3 contents also vary from 3.19 to 3.91, from 0.51 to 0.67, and from 0.14 to 0.26 respectively.

Clinopyroxene from the study area has En, Wo, and Fs values ranging from 48.38 to 49.02, from 46.77 to 48.39, and from 3.23 to 4.76. The amounts of Al_2O_3, Cr_2O_3, TiO_2 and Na_2O vary from 1.72 to 1.79, from 0.60 to 0.69, from 0.04 to 0.06 and from 0.18 to 0.20 respectively. Lherzolite-clinopyroxenes when plotted in the discrimination Mg# vs Al_2O_3 are close to the field of abyssal peridotites and in

Mg# vs Cr_2O_3 diagrams, are close to the field of fore-arc peridotites (Figure 7 a,b).

Spinel chemical analyses are depicted on Table S4 (in Supplementary materials). The Cr# of spinels in harzburgites varies from 29.46 to 44.41 wt%, it is negatively correlated with Mg# values (61.44-77.54) and fall in the field of spinel from abyssal peridotites (Figure 8a). The TiO_2 contents in these spinels are low (0.04 to 0.14 wt%) and do not show a clear correlation with the Cr# (Figure 8b). Al_2O_3 content varies from 29.46 to 49.60 wt% and in the Cr_2O_3 vs Al_2O_3 variation diagram all these Cr-spinels are plotted within the mantle array field (Figure 8c), indicating that they are typical of mantle peridotites with residual character.

Spinels from Abgarm lherzolites have Mg# between 76.00 to 77.23 and Cr# varying from 10.79 to 14.26. TiO_2 content for these spinels varies from 0.02 to 0.05 wt%. In figures (8 a,b) spinels from these rocks settle in the field of spinel from abyssal peridotites with less than 10% partial melting. In the Cr_2O_3 vs Al_2O_3 variation diagram all these Cr-spinels are plotted within the mantle array field (Figure 8c).

Spinels of dunite show a wide variation of Mg# (49.02-53.32) associated with a wide range of Cr# (55.32-76.12) and based on these compositional parameters, the chemistry of chromian spinel is similar to that of spinels in equilibrium with magmas of boninitic affinity (Figure 8a). The TiO_2 amounts are higher (0.16 to 0.21 wt%) than those of harzburgites and approach those of spinels in the chromitite (Figure 8b).

As a whole, spinels of dunite and chromitite show similar compositions, although the latter has slightly lower Cr# contents (63.35-73.78) and higher amounts of Mg# (63.02-69.90), TiO_2 (0.18-0.29 wt%), and Al_2O_3 (12.74-20.89 wt%).

GEOTHERMOBAROMETRY AND OXYGEN FUGACITY

Equilibration pressure and temperature as well as the pressure of the studied Abgram peridotites are based on the compositions of mineral phases. Equilibrium temperatures reported in Table S5 (in Supplementary materials), were calculated using the Ca-orthopyroxene geothermometer of Brey and Kohler (1991) and the geothermometers of Fabriès (1979) and Ballhaus et al. (1991), which are both based on the partitioning of Mg and Fe^{2+} between olivine and spinel. The Brey and Köhler geothermometer provides temperatures in the range of 809-923 °C. However, significantly lower levels of equilibrium temperatures were calculated by Fabriès and Ballhaus et al.'s methods (613-699 °C and 636-725 °C, respectively). The differences in the obtained ranges of temperature equilibrium, which is probably recorded at different times of Abgram peridotites cooling, stems from the difference in the diffusion rates of the mineralogical-systems (Ca-orthopyroxene vs Mg/Fe^{2+} partitioning between olivine and spinel) used for the calculation.

The lack of plagioclase or garnet restricts the pressure of the Abgram peridotites within the spinel stability field, which is within 0.6-0.8 GPa for lherzolite rocks (Borghini et al., 2011) and 3.0 GPa depending on the Cr# of the system (Klemme and O'Neill, 2000). Equilibrium pressure estimates were obtained by the monomineralic geobarometers of Mercier (1980) and Ashchepokov et al. (2010) based on the composition of orthopyroxene and the Cr-spinel, respectively. The equilibration pressure values determined by the Mercier equation are between 1.6 and

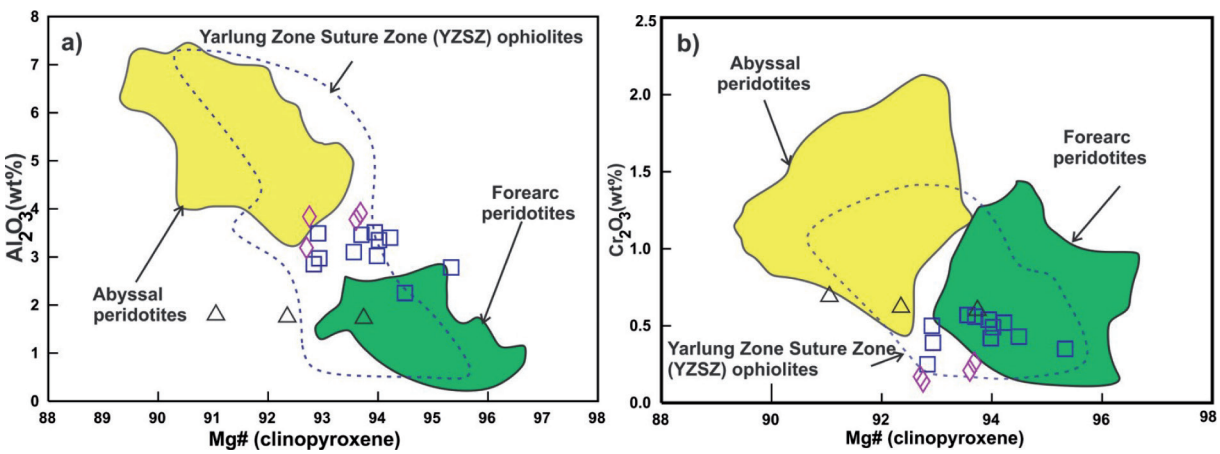

Figure 7. a) Al_2O_3 vs Mg# values in clinopyroxenes. b) Cr_2O_3 vs Mg# values in clinopyroxenes. Data of pyroxene compositions for abyssal and forearc peridotites, as well as those in peridotites from the Yarlung Zangpo Suture Zone (YZSZ) ophiolites, are from the same references used for olivines in Figure 5.

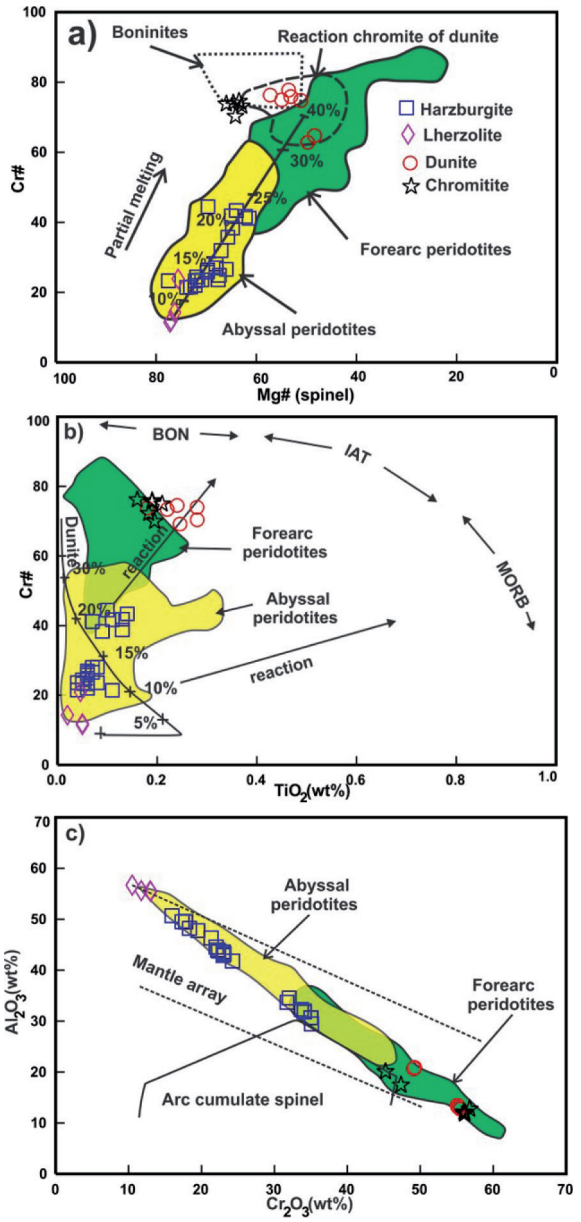

Figure 8. Compositional variation of Cr-spinel of Abgarm peridotites and chromitite. a) Mg# in spinel versus Cr# in Abgarm peridotite; fields are from Kamenetsky et al., (2001). The field for spinel in boninites is taken from Dick and Bullen (1984). The percentage of melting of the host peridotite is after Hirose and Kawamoto (1995); b) TiO_2 versus Cr# diagram after Pearce et al. (2000); c) In Cr_2O_3 versus Al_2O_3 diagram spinels of all peridotite samples plot in the mantle array field and their composition is coherent with the residual character of their harzburgite and dunite host rock. The mantle array and arc cumulate fields are from Conrad and Kay, 1984. Data for spinel in abyssal and forearc peridotites are from Lian et al. (2016, and references therein).

2.1 GPa, while those calculated by the geobarometer of Ashchepokov et al. (2010) vary in the range of 1.1 and 2.3 GPa (Table S5).

The redox state (fO_2) of the samples is reported as Δlog units concerning the fayalite-magnetite-quartz buffer (FMQ); calculations are based on the model of Ballhaus et al. (1991), using the temperatures previously calculated by Ballhaus et al. (1991) geothermometer. Using a uniform equilibration pressure of 1.5 GPa, typical of upper mantle peridotites within the spinel stability field, the calculated fO_2 is in the range Δlog=0.1-0.7 log-bar units for harzburgites and Δlog=0.7 log-bar units for the dunite (Table S5). The use of pressure values calculated by the Cr-spinel geobarometer proposed by Ashchepokov et al. (2010) leads to results that are within uncertainty associated with Ballhaus et al. (1991) oxybarometer (±0.5 log-bar units).

DISCUSSION

Abgarm ultramafic complex contains harzburgites. lherzolite and the dunite including chromitite lenses which are thought to have formed in the upper mantle (Peighambari et al., 2011). Field studies, petrography, and mineral chemistry indicate that the Abgarm peridotites represent the mantle rocks which experienced high degrees of partial melting, high-temperature deformation, and recrystallization processes. In particular, data on modal and/or chemical variability of the peridotites forming-minerals can provide indications on the degree of partial melting, pressure and temperature conditions of rock equilibration and tectonic environments of the peridotites (Dick and Bullen, 1984; Gonzalaz- Jimenes et al., 2011). Whereas, the chemistry of chromian spinel in chromitites provides valuable information on the geochemical signature of the parental magmas from which they were formed (Kamenetsky et al., 2001; Rollinson, 2008 and references therein).

Partial melting of Abgarm mantle peridotites

Modal mineralogy of peridotites and mineral chemical compositions preserve important information on mantle melting process affecting the upper mantle rocks. Clinopyroxene is the most rapidly consumed mineral specifically during the initial stages of partial melting of mantle peridotites, where these minerals systemically decrease as the peridotites become more depleted (i.e., modal clinopyroxene decreases from ~15% in fertile peridotite to 0% in depleted peridotite as the degree of partial melting increases from 0% to ~25% at anhydrous condition; Gaetani and Grove 1998; Parkinson and Pearce 1998). Residual dunite lithology represents a terminal product formed after extensive (to 50-60%) partial melting of peridotite (Mysen and Kushiro, 1977; Bonatti

and Michael, 1989; Kostopoulos, 1991). The mineral chemistry can also be used to evaluate the degree of partial melting of the upper mantle peridotites in ophiolites. For instance, the Al_2O_3 contents of pyroxene and spinel are sensitive to partial melting degrees of mantle rocks, and they systematically decrease as peridotites are more depleted (Dick and Natland, 1996). Further information on the residual degree of mantle peridotites is provided using Mg# (or Fo content in olivine) peridotite minerals as well as by Cr# values of Cr-spinels, which generally increase as the degrees of partial melting increases (Arai, 1994a; Hirose and Kawamoto, 1995). Based on these criteria, the variably depleted nature of Abgarm peridotite rocks is firstly evidenced by their mineralogical composition indicating that they are mantle residues after different degrees of melting. All studied rocks have low clinopyroxene abundance (<5 vol%), which, along with the occurrence of dunites, testify to the high degrees of partial melting suffered by these peridotites. This inference is also supported by the chemical evidence of *i*) the high levels of Fo (90.47 to 91.13) and high values of NiO (0.33 to 0.41%) in olivine crystals (Gaetani and Grove, 1998), *ii*) the Al_2O_3 depletion and the increase of Cr# and Mg# of both orthopyroxenes and clinopyroxenes (Smith and Elthon, 1988) and *iii*) the elevated range of Cr# values in chromian spinel (Figure 8). All these features prove that the Abgarm peridotite complex represents mantle residues after different degrees of partial melting episodes. The extent of such partial melting degrees can be evaluated by mineral chemistry. As stated above, the composition of pyroxenes is a good indicator of the partial melting phenomenon. The Al_2O_3 contents of both orthopyroxene and clinopyroxene Abgarm harzburgites are correlating negatively with MgO abundances; their reciprocal variation is distributed close to the curve representative of an anhydrous melting trend (Upton et al., 2011) indicating a range of partial melting degree of 15-30 % (Figure 9 a,b; Upton et al., 2011). A similar range of melting degrees (10-25%; Figure 8 a,b) is indicated by the composition of Cr-spinels in harzburgites. Conversely, lherzolite shows a partial melting degree lower than 10%; Figure 8a). In addition to the Cr# value of Cr-spinels, the amounts of Fo contents of coexisting olivines are a sensitive indicator of the extent of partial melting of mantle rocks (e.g., Dick and Bullen, 1984; Arai, 1994b). The correlation between the Cr# of spinels and the Fo values of olivines in the Abgarm peridotites reveals that the trend of the analyzed samples is within the olivine-spinel mantle array (OSMA; Arai, 1994b). The aforementioned fact confirms that the Abgarm peridotites are the residues of various degrees of melt extraction ranging between 10 and 20% for harzburgites and 5- 7% for lherzolites (Figure 9c) similar to what was observed for current abyssal peridotites

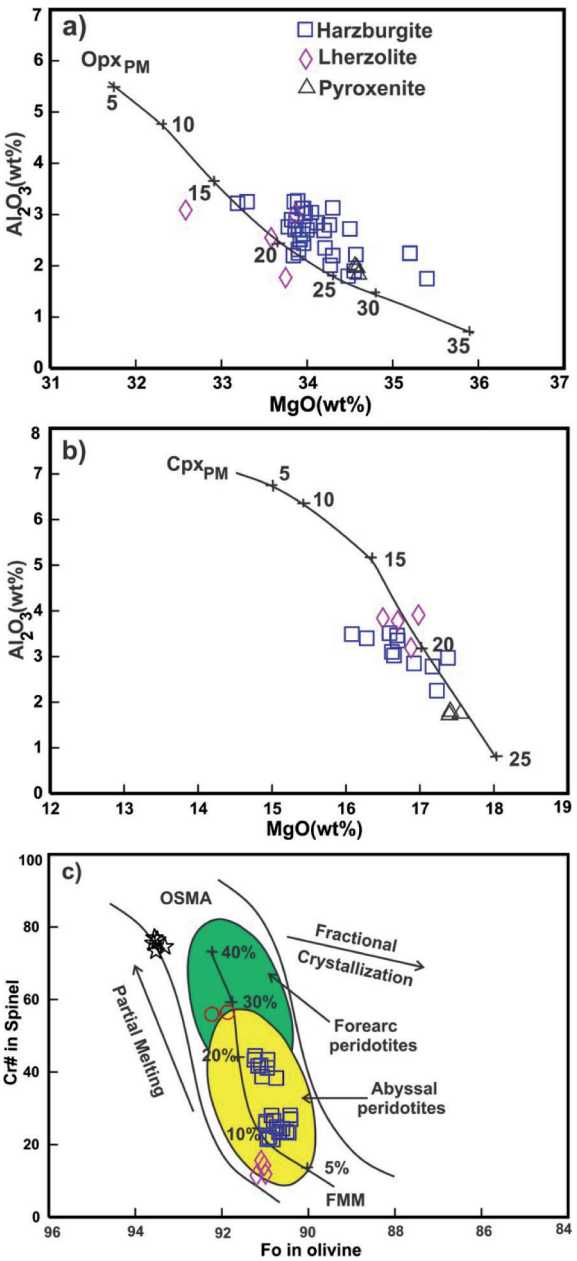

Figure 9. Al_2O_3 and MgO contents variations as function of partial melting degree for a) orthopyroxenes and b) clinopyroxenes of Abgarm harzburgites. The melting curves for both orthopyroxene and clinopyroxene are after Upton et al. (2011). Numbers along the curves correspond to the partial melting percentages; c) Plot of olivine Fo content vs Cr# of coexisting spinel for Abgarm harzburgites and dunite. The olivine-spinel mantle array (OSMA) and melting trend (annotated by melting %) are from Arai (1994b). Fields for abyssal peridotites and forearc peridotites are from Lian et al. (2016, and references therein). FMM-fertile mid-ocean range mantle.

(Khedr and Arai, 2013; Stern et al., 2004). Since the chemical and mineralogical composition of lherzolites is very similar to that of harzburgites, the clinopyroxenes in these rocks may be the product of the reaction of depleted harzburgite with the ascending melt. The chemical composition of chrome-spinels from the harzburgites and lherzolites suggests that they were probably formed in a back-arc basin environment. The dunites and chromitites of the complex can be caused by the reaction of the basaltic melts of the back-arc basin with the mantle peridotites.

Evidences of melt-rock reaction in Abgarm peridotites

The petrographic features and the mineralogical compositions in the investigated Abgarm peridotites cannot be explained only by partial melting mechanisms. Embayed rims of the orthopyroxene porphyroclasts and the secondary small unstrained, replacing minerals within the curved boundaries of these porphyroclasts, are frequently interpreted as a result of a reaction between a percolating melt and peridotite (e.g., Suhr and Edwards, 2000; Zanetti et al., 2006). Furthermore, the formation of dunite in many ophiolite mantle sections is thought to be the result of interaction between infiltrating melts and peridotites, which leads to incongruent pyroxene dissolution and precipitation of olivine and spinel (e.g., Dai et al., 2011).

Changes in the spinel morphology and composition (e.g., Cr# and TiO_2 contents) may also reflect processes such as melt-peridotite reaction during porous flow and melt-wall rock reactions in the vicinity of intruding magmatic veins (Matsumoto and Arai, 2001). For instances, spinel grains in the Abgarm harzburgites do not show the expected negative correlation between Cr# and TiO_2 as a result of the partial melting process (e.g., Pearce et al., 2000; Zhou et al., 2005; Uysal et al., 2007; Delavari et al. 2009). In fact, they demonstrate quite constant TiO_2 contents (0.09-0.14 wt%) with increasing the Cr# values, i.e., the degree of depletion (Figure 8b). In addition, the TiO_2 contents of spinels within the dunite span from that of spinel in the most depleted harzburgite up to overlapping the compositions of the spinels in the chromitite. The displacement from the TiO_2-Cr# melting curve has been interpreted as a consequence of melt mantle interaction through reaction or melt impregnation (Kelemen et al., 1995; Pearce et al., 2000 and references therein). This allows us to infer that the observed TiO_2 enrichment in Abgarm peridotites probably represents the reaction between the preexisting harzburgites and basaltic melts (Figure 8b), from which chromitites were probably crystallized.

Chemical composition of the parental melts of the chromitites

The geochemistry of Cr-spinels in chromitite provides valuable information about the determination of the chemical composition of the parental melt (Arai, 1992; Kamenetsky et al., 2001; Rollinson, 2008). Several studies have shown that FeO/MgO ratio, Al_2O_3 and TiO_2 contents in chromitites, are directly related to parental melt (Dick and Bullen, 1984; Augé, 1987; Arai, 1994a; Zhou et al., 1996; Kamenetsky et al., 2001; Rollinson, 2008). In order to determine the composition of the parental melt of Abgarm, the chromitite values were used the equations proposed by Augé (1987) and Rollinson (2008). The calculated FeO/MgO ratio of the parental melt is between 0.95 and 1.06, while the Al_2O_3 and TiO_2 contents range from 12.16-12.40 wt% and from 0.28 to 0.39 wt%, respectively (Table S4). These calculations were also applied to dunite spinels to estimate the hypothetical composition of melt in equilibrium with these spinels. In Al_2O_3 vs TiO_2 diagram, the parental melts determined of both chromitite and dunite samples are plotted close to boninites area and within the field defined by the composition of calculated parental of chromitites from the same Esfandagheh-Hajiabad district (Figure 10).

Tectonic setting of the Abgarm peridotite section

Ophiolites formation was usually related to mid-ocean ridge spreading centers, however, recent studies of modern oceanic basins demonstrated the influence of subduction on the formation of ophiolitic sequences known as the supra-subduction zone (SSZ) ophiolites (Dilek and Furnes, 2014; Stern et al., 2012 and references therein). Worldwide well-preserved ophiolites show both MOR and SSZ mantle compositions (Pearce et al.,

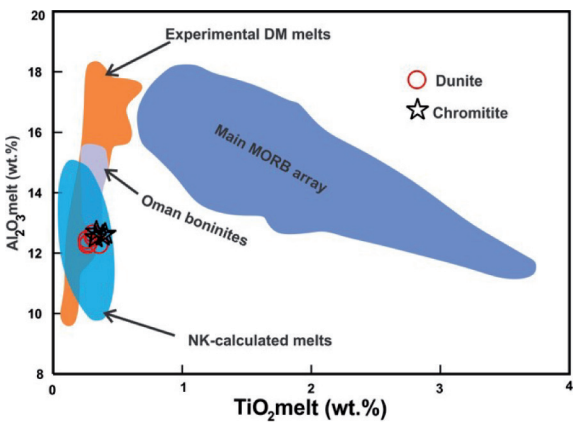

Figure 10. TiO_2 vs Al_2O_3 variation diagram of calculated melts in equilibrium with the Cr-spinels of chromitite and dunite. The field of the main MORB array and composition melt calculations are based on Rollinson (2008). Field of the Oman boninites from Ishikawa et al. (2002), and melts of the depleted mantle (DM) are from Schwab and Johnston (2001). NK=Nazdasht chromitite pods (Colkahan ultramafic complex, Haji Abad-Esfandagheh district, Kerman province; Najafzadeh, 2017).

1984; Stern, 2004) and in the fore-arc regions, mantle peridotites are known to contain both SSZ and abyssal peridotites (Parkinson and Pearce, 1998; Pearce et al., 2000). As stated in previous sections, the composition of Cr-spinels, joint to the elemental and modal compositions of the mineral constituents of mantle peridotites, is a good indicator of the tectono-magmatic history of the host rock (e.g., Dick and Bullen, 1984; Arai, 1992; Zhou et al., 2005; Arai et al., 2011; Ahmed et al., 2012; Uysal et al., 2012).

Petrography and geochemistry of the Abgarm peridotites samples provide clear evidence that the upper mantle of this area was affected by a multi-process history. Overall, the mineral chemistry of the studied harzburgites falls in the abyssal peridotite fields in the discrimination diagrams, tending towards the forearc region increasing the residual character of these rocks (Figures 5,6,7,8). Moreover, because the TiO_2 content of chromian spinels is considered a key factor for the identification of the geodynamic setting (e.g. Arai and Matsukage, 1998; Bonavia et al., 1993), the Al_2O_3 vs TiO_2 diagram (Figure 11) can be used to better define the tectonic setting(s), in which Abgarm Cr-spinels were formed. In this diagram, Cr-spinels from harzburgites are plotted between the MORB-type and SSZ-type peridotite fields; Cr-spinels from lherzolites occur in MORB-type peridotites. Whereas, chromites from dunites and chromitite pods fall in the SSZ- peridotite fields close to the back-arc basin field (Figure 11) suggesting that Cr-spinels of the most depleted harzburgites were modified by reaction with boninitic melts (see also previous sections). In the fore-arc region, peridotites are commonly affected by a combination of processes including partial melting and metasomatism, as is the case for the investigated peridotites, implying a two-stage formation process and evolution of the Abgarm peridotites. In this model, MORB-type peridotites were trapped above an intra-oceanic subduction zone as the part of the mantle wedge and their compositions were variably changed by upward-moving boninitic fluids and melt during the subduction stage. This interpretation could also be applicable to the dunite samples, in which the estimated parental melt of chromites shows boninitic characteristics. The reaction between the depleted harzburgites and the basaltic melts could have also converted some of the Abgarm harzburgites to dunites. Previous studies on Kermanshah ophiolites (e.g., Seccani et al., 2013) and Haji Abad-Esfandagheh ophiolites (e.g. Moghadam et al., 2013; Mohammadi et al., 2018; Najafzadeh, 2017) suggested a fore-arc tectonic setting for the generation of the magmatic rocks in the southern branch of Neotethys during the Late Cretaceous. The present study shows that the Abgarm peridotites may have been formed in a back-arc setting environment.

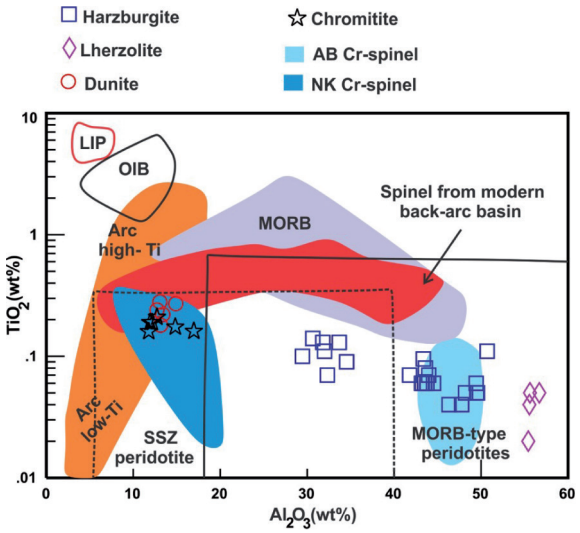

Figure 11. TiO_2 vs Al_2O_3 diagram for chrome-spinels of the Abgarm peridotites and chromite concerning modern-day tectonic settings (modified after Najafzadeh, 2017). The fields are from Kamenetsky et al. (2001). SSZ supra-subduction zone; LIP large igneous province; MORB mid-ocean ridge basalt; OIB ocean island basalt. The high-Ti IAB (High-K calc-alkaline suite) is divided from low-Ti IAB (boninite and low-Ti tholeiite suites) by the thick dashed line at TiO_2=0.3 wt%. NK= Nazdasht Cr-spinels of peridotites (harzburgites and dunites) and chromitite pods (Colkahan ultramafic complex, Haji Abad-Esfandagheh district, Kerman province; Najafzadeh, 2017). AB=Cr-spinels from peridotites of Ab-Bid ultramafic complex (Haji Abad-Esfandagheh district, Kerman province Mohammadi et al., 2018).

CONCLUSIONS

Field relations, petrographic and geochemical characteristics of Abgarm peridotites reported here for the first time, indicate that:

1- The ultramafic bodies of the Abgarm complex are dominated by harzburgite with minor dunites; some of the dunites contain massive chromite pods or bands. The peridotites samples have protogranular to porphyroclastic textures with different generations of minerals.

2- Mineralogical and geochemical heterogeneities of these rocks are due to differences in the degree of their residual character coupled with the effects of interaction between harzburgites and magmas with basaltic affinity.

3- Geothermo-barometric estimates indicate that the harzburgitic Abgarm mantle has initially been equilibrated at temperatures between 809-923 °C and then at 613-725 °C, in a range of pressures of 1.1 and 2.3 GPa. Moreover, fO_2 calculation gives a redox state that lies within a range of 0.7 log bar units around the fayalite-magnetite-quartz buffer FMQ (Δlog=0.1-0.7 log-bar units).

4 - The calculated average Al_2O_{3melt} and TiO_{2melt} values

for the chromitites pods are ~12 wt% and ~0.4 wt%, consistent with a parental melt of basaltic affinity found in forearc settings. A basaltic melt can be the cause of compositional variations in Cr-spinels of the dunites.

5 - Abgarm ultramafic complex preserve evidence for the evolution of Neotethys oceanic lithosphere in South of Iran, which involves partial melting of abyssal peridotites and fertilization processes in the supra-subduction zone environment.

ACKNOWLEDGEMENTS

We thank D. Mannetta (Dipartimento Scienze Della Terra, Sapienza Università di Roma) for his help in preparing the petrographic thin sections of the selected rocks for analyses, M. Albano (CNR-IGAG) and M. Serracino (CNR-IGAG) for their assistance during SEM and EPMA analytical sessions. This research has been financially supported by a grant from the Shahid Bahonar University of Kerman. In addition, the authors are grateful to Prof. Nakashima for his support with microprobe analyses at the Yagamata university of Japan.

REFERENCES

Agard P., Monie P., Gerber W., Omrani J., Molinaro M., Meyer B., Labrousse L., Vrielynck B., Jolivet L., Yamato P., 2006. Transient, syn-obduction exhumation of Zagros blueschists inferred from P-T-deformation-time and kinematic constraints: implications for Neotethyan wedge dynamics. Journal of Geophysical Research 111, B11401.

Ahmadipour H., Sabzehei M., Whitechurch H., Rastad E., Emami M.H., 2003. Soghan complex as an evidence for paleospreading center and mantle diapirism in sananandaj-sirjan zone (South-East Iran). Journal of Sciences, Islamic Republic of Iran 14, 157-172.

Ahmed H.A., Harbi H.M., Habtoor A.M., 2012. Compositional variations and tectonic settings of podiform chromitites and associated ultramafic rocks of the Neoproterozoic ophiolite at Wadi Al Hwanet, northwestern Saudi Arabia. Journal of Asian Earth Sciences 56, 118-134.

Ahmed A.H., 2013. Highly depleted harzburgite-dunite-chromitite complexes from the Neoproterozoic ophiolite, south Eastern Desert, Egypt: a possible recycled upper mantle lithosphere. Precambrian Research 233,173-192.

Alipour R., Moeinzadeh H., Ahmadipour H., 2021a. Mineral chemistry studies of dunites in the Abgarm region (south of Kerman province): An approach to tectonomagmatic position. Journal of Crystallography and Mineralogy in persian.

Alipour R., Moeinzadeh H., and Ahmadipour H., 2021b. Spinel mineralogy evidence to determine the origin of Abgarm ultramafic complex (South of Kerman province). Journal of Petrology in persian.

Arai S., 1992. Chemistry of Chromian spinel in volcanic rocks as a potential guide to magma chemistry. Mineralogical Magazine 56, 173-184.

Arai S.,1994a. Characterization of spinel peridotites by olivine-spinel compositional relationships: review and interpretation. Chemical Geology 113, 191-204.

Arai S., 1994b. Compositional variation of olivine-chromian spinel in Mg-rich magma as guide to their residual spinel peridotites. Journal of Volcanology and Geothermal Research 59, 279-293.

Arai S. and Matsukage K., 1998. Petrology of a chromitite micropod from Hess deep, equatorial Pacific: a comparison between abyssal and alpine-type podiform chromitites. Lithos 43, 1-14

Arai S., Okamura H., Kadoshima K., Tanaka C., Suzuki K., Ishimaru S., 2011. Chemical characteristics of chromian spinel in plutonic rocks: implications for deep magma processes and discrimination of tectonic setting. Island Arc 20, 125-137.

Arvin M. and Robinson P.T., 1994. The petrogenesis and tectonic setting of lavas from the Baft ophiolitic mélange, southwest of Kerman, Iran. Journal of Volcanology and Geothermal Research 31, 824-834.

Ashchepkov I.V., Pokhilenko N.P., Vladykin N.V., Logvinova A.M., Kostrovitsky S.I., Afanasiev V.P., Pokhilenko L.N., Kuligin S.S., Malygina L.V., Alymova N.V., Khmelnikova O.S., Palessky S.V., Nikolaeva I.V., Karpenko M.A., Stegnitsky Y.B., 2010. Structure and evolution of the lithospheric mantle beneath Siberian craton, thermobarometric study. Tectonophysics 485, 17-41.

Auge T., 1987. Chromite deposits in the northern Oman ophiolite: mineralogical constraints. Mineralium Deposita 22, 1- 10.

Ballhaus C., Berry R.F., Green D.H., 1991. High pressure experimental calibration of the olivine-orthopyroxene-spinel oxygen geobarometer: implications for the oxidation state of the upper mantle. Contributions to Mineralogy and Petrology 107, 27-40.

Bonatti E. and Michael P.J., 1989. Mantle peridotites from continental rifts to ocean basins to subduction zones. Earth and Planetary Science Letters 91, 297-311.

Bonavia F., Diella V., Ferrario A., 1993. Precambrian podiform chromitites from Kenticha Hill, southern Ethiopia. Economic Geology 88, 198-202.

Borghini G., Fumagalli P., Rampone E., 2011. The geobarometric significance of plagioclase in mantle peridotites: A link between nature and experiments. Lithos 126, 42-53.

Brey G.P. and Kohler T., 1991. Geothermobarometry in four-phase lherzolites. Part ll: New thermobarometers and practical assessment of existing thermobarometers. Journal of Petrology 31, 1353-1309.

Conrad W.K. and Kay R.W., 1984. Ultramafic and mafic inclusions from Adak Island: crystallisation history and implications for the nature of primary magmas and crustal evolution in the Aleutian arc. Journal of Petrology 25, 99-125.

Dai J.G., Wang C-S., Hébert R., Santosh M., Li Y-L, Xu J-Y.,

2011. Petrology and geochemistry of peridotites in the Zongba Ophiolite, Yarlung Zangbo Suture Zone: implications for the Early Cretaceous intra-oceanic subduction zone within the Neo-Tethys. Chemical Geology 288, 133-148.

Dai J., Wang C., Polat A., Santosh M., Li Y., Ge Y., 2013. Rapid forearc spreading between 130 and 120 Ma: evidence from geochronology and geochemistry of the Xigaze ophiolite, southern Tibet. Lithos 172-173,1-16.

De Hoog J.C.M., Gall L., Cornell D., 2010. Trace element geochemistry of mantle olivine and applications to mantle petrogenesis and geothermobarometry. Chemical. Geology 270, 196-215.

Delavari M., Amini S., Saccani E., Beccaluva L., 2009. Geochemistry and petrogenesis of mantle peridotites from the Nehbandan Ophiolitic Complex, Eastern Iran. Journal of Applied Science 15, 2671-2687.

Dick H.J.B. and Bullen T., 1984. Chrome spinel as a petrogenetic indicator in abyssal and alpine-type peridotites and spatially associated lavas. Contributions to Mineralogy and Petrology 86, 54-76.

Dick H.J.B. and Natland J.H., 1996. Late-stage melt evolution and transport in the shallow mantle beneath the east Pacific rise. In: Mevel, C., Gillis, K.M., Allan, J.F., and Meyer, P.S., (eds.), Proceedings of the Ocean Drilling Program, Scientific Results, 47, Ocean Drilling Program, College Station, TX, 103-341.

Dilek Y. and Furnes H., 2009. Structure and geochemistry of Tethyan ophiolites and their petrogenesis in subduction rollback systems. Lithos 113, 1-20.

Dilek Y. and Furnes H., 2014. Ophiolites and their origins. Elements 10, 93-100.

Dilek Y. and Thy P., 2009. Island arc tholeiite to boninitic melt evolution of the Cretaceous Kızıldağ (Turkey) ophiolite: model for multistage early arc-forearc magmatism in Tethyan subduction factories. Lithos 113, 69-90.

Dupuis C., Hébert R., Dubois-Côté V., Guilmette C., Wang C.S., Li Y.L., Li Z.J., 2005. The Yarlung Zangbo Suture Zone ophiolite mélange (southern Tibet): new insights from geochemistryof ultramafic rocks. Journal of Asian Earth Sciences 25, 937-960.

Fabries I., 1979. Spinel-olivine geothermometry in peridotites from ultramafic complexes. Contributions to Mineralogy and Petrology 69, 329-336.

Gaetani G. A. and Grove T. L., 1998. The influence of water on melting of mantle peridotite. Contributions to Mineralogy and Petrology 131, 323-346.

Ghasemi H., Juteau T., Bellon H., Sabzehei M., Witechurch H., Ricou L.M., 2002. The mafic-ultramafic complex of Sikhoran (central Iran): a polygenetic ophiolitic complex. Geoscience 334, 431-439.

González-Jiménez J.M., Proenza J.A., Gervilla F., Melgarejo J.C., BlancoMoreno J.A., Ruiz-Sánchez R., Griffin W.L., 2011. High-Cr and High-Al chromitites from the Sagua de Tánamo district, Mayarí Cristal ophiolitic massif (eastern Cuba): constraints on their origin from mineralogy and geochemistry of chromian spinel and platinum-group elements. Lithos 125, 101-121.

Hirose K. and Kawamoto T., 1995. Hydrous partial melting of lherzolite at 1GPa: the effect of H_2O on the genesis of basaltic magmas. Earth and Planetary Science Letters 133, 463-473.

Ishikawa T., Nagaishi K., Umino S., 2002. Boninitic volcanism in the Oman ophiolite: implications for thermal condition during transition from spreading ridge to arc. Geology 30, 899-902.

Jannessary M-R., Melcher F., Lodziak J., Meisel TH-C., 2012. Review of platinum-group element distribution and mineralogy in Chromitite ores from southern Iran, Ore Geology 49, 209-325.

Kamenetsky V.S., Crawford A.J., Meffre S., 2001. Factors controlling chemistry of magmatic spinel: an empirical study of associated olivine, Cr-spinel and melt inclusions from primitive rocks. Journal of Petrology 42, 655-671.

Kelemen P.B., Dick H.j.B., Quick J.E., 1992. Formation of harzburgite by pervasive melt/rock reaction in the upper mantle. Nature 359, 635-641.

Kelemen P.B., Shimizu N., Salters V.J.M., 1995. Extraction of mid-ocean ridge basalt from the upwelling mantle by focused melt in dunite channels. Nature 375, 747-753.

Khalatbari Jafari M., Babaie H.A., Moslempour M.E., 2016, Mid-ocean-ridge to suprasubduction geochemical transition in the hypabyssal and extrusive sequences of major Upper Cretaceous ophiolites of Iran. In: Tectonic Evolution, Collision, and Seismicity of Southwest Asia: In Honor of Manuel Berberian's Forty-Five Years of Research Contributions. (Ed.): R. Sorkhabi, Geological Society of America Special Paper 525, 229-289.

Khedr M.Z. and Arai S., 2013. Origin of Neoproterozoic ophiolitic peridotites in south Eastern Desert, Egypt, constrained from primary mantle mineral chemistry. Mineralogy and Petrology 107, 807-828.

Klemme S. and O'Neill H.S., 2000. The near-solidus transition from garnet lherzolite to spinel lherzolite. Contributions to Mineralogy and Petrology 138, 237-248.

Kostopoulos D., 1991. Parameterization of the melting regime of the shallow upper mantle and the effects of variable lithospheric stretching on mantle modal stratification and trace-element concentrations in magmas. Journal of Petrology 33, 665-691.

Le Maitre R.W., 1989. A classification of igneous rocks and glossary of terms. Recommendations of the IUGS Commission on the systematics of igneous rocks. Oxford: Blackwell.

Lian D., Yang J., Robinson P.T., Liu F., Xiong F., Zhang L., Gao J., Wu W., 2016. Tectonic evolution of the western Yarlung Zangbo Ophiolitic Belt, Tibet: implications from the petrology, mineralogy, and geochemistry of peridotites. Journal of Geology 124, 353-376.

Lian D., Yang J., Dilek Y., Rocholl A., 2019. Mineralogy and geochemistry of peridotites and chromitites in the Aladag Ophiolite (southern Turkey): melt evolution of the Cretaceous Neotethyan mantle. Journal of the Geological Society 176, 958-974.

MatSumoto I. and Arai S., 2001. Morphological and chemical variations of chromian spinel in dunite-harzburgite complexes from the Sangun Zone (SW Japan): implications for mantle/melt reaction and chromitite formation processes. Mineralogy and Petrology 73, 305-323.

Mercier J-C.C., 1980. Single-pyroxene thermobarometry. Tectonophysics 70, 1-37

Mohammadi M.H., Ahmadipour H., Moradian A., 2018. Origin of Lherzolitic Peridotites in Ab-Bid Ultramafic Complex (Hormozgan Province); Products of Mantle Metasomatism or Partial Melting Processes? Journal of Sciences, Islamic Republic of Iran 29, 53-65

Moghadam H.S., Stern R.J., Chiaradia M., Rahgoshay M., 2013. Geochemistry and tectonic evolution of the Late Cretaceous Gogher-Baft ophiolite, Central Iran. Lithos 168-169, 33-47

Moores E.M., Kellogg L.H., Dilek Y., 2000. Tethyan ophiolites, mantle convection, and tectonic ‘‘historical contingency’’; a resolution of the ‘‘ophiolite conundrum’’. In: Dilek Y., Moores E.M., Elthon D., Nicolas A. (Eds.), Ophiolites and Oceanic Crust: New Insights from Field Studies and the Ocean. Drilling Program: Geological Society of America Special Paper, 349 pp.

Mysen B.O. and Kushiro I., 1977. Compositional Variations of Coexisting Phases with Degrees of Melting of Peridotite in the Upper Mantle. American Mineralogist 62, 843-865.

Najafzadeh A.R. and Ahmadipour H., 2014. Using platinum-group elements and Au geochemistry to constrain the genesis of podiformchromitites and associated peridotites from the Soghan mafic-ultramafic complex, Kerman, southeastern Iran. Ore Geology Reviews 62, 62-75.

Najafzadeh A.R., 2017. Mineralogy and composition of chromitites and host peridotites from the Colkahan ultramafic complex (Nazdasht mine), Kerman, southeastern Iran. Mineralogy and Petrology 111, 337-350

Niu Y., 2004. Bulk-rock major and trace element compositions of abyssal peridotites: implications for mantle melting, melt extraction and post-melting processes beneath mid-ocean ridges. Journal of Petrology 45, 2423-2458.

Parkinson I.J. and Pearce J.A., 1998. Peridotites from the Izu-Bonin- Mariana forearc (ODP Leg 125): evidence for mantle melting and melt-mantle interactions in a supra-subduction zone setting. Journal of Petrology 39, 1577-1618.

Pearce J.A., Lippard S.J., Roberts S., 1984. Characteristics and tec- tonic significance of supra-subduction ophiolites. In: Marginal Basin Geology. (Eds.): B.P. Kokelaar and M.F. Howells, Geological Society, London, Special Publications, 16, 777-794.

Pearce J.A., Barker P.F., Edwards S.J., Parkinson I.J., Leat P.T., 2000. Geochemistry and tectonic significance of peridotites from the South Sandwich arc-basin system, south Atlantic. Contribution to Mineralogy and Petrology 139,36 -53.

Pearce J.A. and Robinson P.T., 2010. The Troodos ophiolite complex probably formed in a subduction initiation, slab edge setting. Gondwana Research, 18, 60-81.

Peighambari S., Ahmadipour H., StoschH G., Daliran F., 2011. Evidence for multi-stage mantle metasomatism at the Dehsheikh peridotite mass if and chromite deposits of the Orzuieh coloured mélange belt, southeastern Iran, Ore Geology Reviews, 32, 245-264.

Pelletier L., Vils F., Kalt A., Gmeling K., Li., 2008. Li and Be contents of harzburgites from the Dramala Complex (Pindos ophiolite, Greece): Evidence for a MOR-type mantle in a supra-subduction zone environment. Journal of Petrology 49, 2043- 2080.

Pouchou J.L. and Pichoir F., 1991. Quantitative analysis of homogeneous or stratified microvolumes applying the model “PAP”. In: Heinrich, K.F.J., Newbury, D.E. (Eds.), Electron Probe Quantitation. Plenum, New York, pp. 31-75.

Pouchou J.L. and Pichoir F., 1991. Quantitative analysis of homogeneous or stratified microvolumes applying the model “PAP”. In: Heinrich, K.F.J., Newbury, D.E. (Eds.), Electron Probe Quantitation. Plenum, New York, 31-75.

Robertson A.H.F., 2002. Overview of the genesis and emplacement of Mesozoic ophiolites in the Eastern Mediterranean Tethyan region. Tectonophysics 65, 1-67.

Rollinson H., 2008. The geochemistry of mantle chromitites from the northern part of the Oman ophiolite: inferred parental melt compositions. Contribution to Mineralogy and Petrology 156, 273-288.

Saccani E., Khalil Allahyari K., Beccaluva L., Gianluca Bianchini G., 2013. Geochemistry and petrology of the Kermanshah ophiolites (Iran): Implication for the interaction between passive rifting, oceanic accretion, and OIB-type components in the Southern Neo-Tethys Ocean Gondwana Research 24, 392-411.

Sahandi M.R., Azizian H., Nazemzade M., Navazi M., Atapour H., 2007. 1/10000 level orzueiyeh Geological map. Geological Survey & Mineral exploration of Iran, Series, No. 7346.

Schwab B.E. and Johnston A.D., 2001. Melting systematics of modally variable, compositionally intermediate peridotites and the effects of mineral fertility. Journal of Petrology 42, 1789-1811.

Shafaii Moghadam H., Mosaddegh H., Santosh M., 2012. Geochemistry and petrogenesis of the Late Cretaceous Haji-Abad ophiolite (outer Zagros Ophiolite Belt, Iran): implications for geodynamics of the Bitlis-Zagros suture zone. Geological Journal 48, 579-602.

Shafaii Moghadam H., Stern R.J., 2015. Ophiolites of Iran: keys to understanding the tectonic evolution of SW Asia: (I) Paleozoic ophiolites. Journal of Asian Earth Science 91, 19-38.

Singh A.K., Nayak R., Khogenkumar S., Subramanyam K.S.V.,

Thakur S.S., Singh R.K.B., Satyanarayanan M., 2017. Genesis and tectonic implications of cumulate pyroxenites and tectonite peridotites from the Nagaland-Manipur ophiolites, Northeast India: constraints from mineralogical and geochemical characteristics, Geological Journal 52, 415-436.

Smith S.E. and Elthon D., 1988. Mineral compositions of plutonic rocks from the Lewis Hills Massif, Bay of Islands ophiolite. Journal of Geophysical Research 93, 3450-3468.

Stern R.J., Johnson P.R., Kröner A., Yibas B., 2004. Neoproterozoic ophiolites of the Arabian-Nubian Shield. In: Precambrian ophiolites and related rocks. (Ed.): Kusky T.M. Developments in Precambrian geology, vol 13. Elsevier, Amsterdam, 95-128.

Stern R.J.M., Reagan M., Ishizuka O., Ohara Y., Whattam S., 2012. To understand subduction initiation, study forearc crust: To understand forearc crust, study ophiolites. Lithosphere 4, 469-483.

Suhr G. and Edwards J.E., 2000. Contrasting mantle sequences exposed in the Lewis Hill massif: evidence for early, arc-related history of the Bay of Islands ophiolite. Geological Society of America Special Paper 349, 433-442.

Upton B.G.J., Downes H., Kirstein L.A., Bonadiman C., Hill P.G., Ntaflos T., 2011. The lithospheric mantle and lower crust-mantle relationships under Scotland: a xenolithic perspective. Journal of the Geological Society 168, 873-886.

Uysal I., Kaliwoda M., Karsli O., Tarkian M., Sadiklar M.B., Ottley C.J., 2007. Compositional variations as a result of partial melting and malt-peridotite interaction in an Upper mantle section from the Ortaca area, Southwestern Turkey. The Canadian Mineralogist 45, 1401-1423.

Uysal I., Ersoy E.Y., Karsli O., Dilek Y., Burthan Sadiklar M., Ottley C.J., Tiepolo M., Meisel T., 2012. Coexistence of abyssal and ultra-depleted SSZ type mantle peridotites in a neo-Tethyan ophiolite in SW Turkey: constraints from mineral composition, whole-rock geochemistry (major-rare-REE-PGE), and Re-Os isotope systematics. Lithos 132-133, 50-69.

Uysal I., Ersoy E.Y., Dilek Y., Kapsiotis A., Sarifakioglu E., 2016. Multiple episodes of partial melting, depletion, metasomatism and enrichment processes recorded in the heterogeneous upper mantle sequence of the Neotethyan Eldivan ophiolithe (Turkey). Lithos 246-247, 228-245.

Weber-Diefenbach K., Davoudzadeh M., Alavi-Tehrani N., Linsch G., 1984. Paleozoic ophiolites in Iran, Geology and geochemistry, and geodynamic implication. Ofioliti 11, 305-383.

Zanetti A., D'Antonio M., Spadea P., Raffone N., Vannucci R., Brugeir O., 2006. Petrogenesis of mantle peridotites from the Izu-Bonin-Mariana (IBM) forearc. Ofioliti 31, 189-206.

Zhang L., Yang J.S., Liu F., Lian D.Y., Huang J., Zhao H., Yang Y., 2016. The South Gongzhucuo peridotite massif: A typical MOR type peridotite in the western Yarlung Zangbo suture zone. Acta Petrologica Sinica 32, 3649-3672.

Zhou M.F., Robinson P.T., Malpas J., Li Z., 1996. Podiform chromitites in the Luobusa ophiolite (southern Tibet): implications for melt-rock interaction and chromite segregation in the upper mantle. Journal of Petrology 37, 3-21.

Zhou M.F., Robinson P.T., Lesher C.M., Keays R.R., Zhang C.J., Malpas J., 2005. Geochemistry, petrogenesis, and metallogenesis of the Panzhihua gabbroic layered intrusion and associated Fe- Ti- V- oxide deposits, Sichuan Province, SW China. Journal of Petrology 46, 2253-2280.